Supporting Information

Wisitsorasak and Wolynes 10.1073/pnas.1214130109

SI Text

Derivation of Eq. 4. At low temperature near T_K the RFOT theory of glasses predicts that the cooperatively rearranging regions (CRRs) in glass-forming liquids are compact. Away from T_K, CRRs need not be compact and string-like contiguous shapes, called lattice animals, have been observed in computer simulations and experiments. Accouting for the multiplicity of possible shapes of the CRRs (1) and using the landscape library arguments (2), the free energy of a CRR of N sites with b boundary interactions is

$$F(N,b,\sigma) = [f_{\rm eq}(T) - \phi_{\rm in}(T,\sigma)]N + v_{\rm int}b - k_{\rm B}T\ln\Omega(N,b) \quad \textbf{[S1]}$$

where $f_{\rm eq}(T)$ is the total bulk free energy per particle of an equilibrium state at temperature T, $\phi_{\rm in}(T)$ is the internal free energy per particle of an initial glass state, $v_{\rm int} = (1/z)T_K(3/2)k_{\rm B}\ln(\alpha_L a^2/\pi e)$ is a local interaction of pairs with z nearest neighbors, and $\Omega(N,b)$ is the number of lattice animals of given N and b. The initial nonequilibrated free energy has an additional contribution due to stress

$$\phi_{\rm in}(T,\sigma) = \phi^0_{\rm in}(T) + \kappa\frac{\sigma^2}{2G}V_{\rm bead} \quad \textbf{[S2]}$$

where $\phi^0_{\rm in}$ is an internal free energy of the initial state without any stress. The equilibrated bulk free energy at temperature T above T_K is the sum of the internal free energy of a state at the Kauzmann temperature T_K and the configurational entropy s_c

$$f_{\rm eq}(T) = \phi_K - \int_{T_K}^{T} dT' s_c(T') \quad \textbf{[S3]}$$

$$= \phi_K - \Delta c_p(T_g)T_g\left(\frac{T-T_K}{T_K} - \ln\frac{T}{T_K}\right) \quad \textbf{[S4]}$$

where we have used Angell's empirical form of the change in heat capacity upon vitrification $\Delta c_p(T) = \Delta c_p(T_g)(T_g/T)$ and the thermodynamic relation, $s_c(T) = \int_{T_K}^{T} dT' \frac{\Delta c_p(T')}{T'} = \Delta c_p(T_g)T_g(\frac{1}{T_K} - \frac{1}{T})$. Note that $f_{\rm eq}(T_g) = \phi_g - T_g s_c(T_g)$. The ideal glass state energy is equal to

$$\phi_K = \phi_g - \Delta c_p(T_g)T_g\ln\frac{T_g}{T_K}. \quad \textbf{[S5]}$$

Consider the first term on the right-hand side of Eq. **S1** and let $\phi^0_{\rm in}(T)$ be the bulk energy at T_g. Then use the relation in Eq. **S5** to obtain

$$f_{\rm eq}(T) - \phi_{\rm in}(T,\sigma) = -\Delta c_p(T_g)T_g\left\{\frac{T-T_K}{T_K} + \ln\frac{T_g}{T}\right\} - \kappa\frac{\sigma^2}{2G}V_{\rm bead}. \quad \textbf{[S6]}$$

Substitute this result back into Eq. **S1**. The free energy becomes

$$F(N,b,\sigma) = \left[-\Delta c_p(T_g)T_g\left\{\frac{T-T_K}{T_K} + \ln\frac{T_g}{T}\right\} - \kappa\frac{\sigma^2}{2G}V_{\rm bead}\right]N + v_{\rm int}b - k_{\rm B}T\ln\Omega(N,b). \quad \textbf{[S7]}$$

If T is below T_K, the excess energy is frozen at the state $T = T_K$ and the configurational entropy vanishes

$$F(N,b,\sigma) = \left[-\Delta c_p(T_g)T_g\ln\frac{T_g}{T_K} - \kappa\frac{\sigma^2}{2G}V_{\rm bead}\right]N + v_{\rm int}b - k_{\rm B}T\ln\Omega(N,b). \quad \textbf{[S8]}$$

In percolation clusters (3), for large N, the number of lattice animals is approximately

$$\Omega_{\rm perc} \equiv \left(\frac{(\alpha+1)^{\alpha+1}}{\alpha^\alpha}\right)^N \exp\left(-\frac{N^{2\phi}}{2B^2}(\alpha-\alpha_e)^2\right) \quad \textbf{[S9]}$$

where $\alpha = t/N$, and t is the number of unoccupied sites bounding the occupied cluster. Follow the analysis by Stevenson, Schmalian, and Wolynes (1) in which $v_{\rm int}b$ and $k_{\rm B}T\ln\Omega_{\rm perc}$ are carried out explicitly, we take the exponent ϕ at mean field value of 1/2 and a lattice constant $B = 1.124$. The number of bonds b is directly related to t and should linearly depend on coordination number $b \approx 1.68tz/z_{\rm SC}$ (4), where $z_{\rm SC}$ is the coordination number for the simple cubic lattice. Recall that the interaction energy $v_{\rm int} = (1/z)T_K(3/2)k_{\rm B}\ln(\alpha_L a^2/\pi e) = 3.6907k_{\rm B}T_K/z$. The free energy in Eq. **S8** is now a function of N and t. Minimize this function with respect to t, the most probable value of t is $\bar{t} = \bar{\alpha}N$, where $\bar{\alpha} = 3.10$ at $T = T_K$. At this most probable value, $\Omega_{\rm perc}$ becomes a simple exponential function, $\Omega_{\rm perc} \sim \lambda^N$, where $\lambda = 6.82$. Each term in Eq. **S8** is now proportional to N, and we can write

$$F(N,b,\sigma) = \left[-\Delta c_p(T_g)T_g\ln\frac{T_g}{T_K} - \kappa\frac{\sigma^2}{2G}V_{\rm bead}\right]N + v_{\rm int}1.68\frac{z_{fcc}}{z_{\rm SC}}\bar{\alpha}N - k_{\rm B}TN\ln\lambda \quad \textbf{[S10]}$$

$$= k_{\rm B}TN\left\{\left[-\frac{\Delta c_p(T_g)}{k_{\rm B}}\frac{T_g}{T}\left\{\ln\frac{T_g}{T_K}\right\} - \frac{1}{k_{\rm B}T}\frac{\kappa\sigma^2}{2G}V_{\rm bead}\right] + \frac{v_{\rm int}}{k_{\rm B}T}1.68\frac{z_{f.c.c.}}{z_{\rm SC}}\bar{\alpha} - \ln\lambda\right\}. \quad \textbf{[S11]}$$

At the thresholding stress σ^* where $F(N,\sigma^*) = 0$, one finds

$$\sigma^* = \sqrt{\frac{2Gk_{\rm B}T}{\kappa V_{\rm bead}}\left(\left[\frac{v_{\rm int}}{k_{\rm B}T}1.68\frac{z_{f.c.c.}}{z_{SC}}\bar{\alpha} - \ln\lambda\right] - \frac{\Delta c_p(T_g)}{k_{\rm B}}\frac{T_g}{T}\ln\frac{T_g}{T_K}\right)}, \quad \textbf{[S12]}$$

or

$$\sigma^* = \sqrt{\frac{2Gk_{\rm B}T}{\kappa V_{\rm bead}}\frac{v_{\rm int}}{k_{\rm B}T}\left(1.68\frac{z_{f.c.c.}}{z_{\rm SC}}\bar{\alpha} - \left[\ln\lambda + \frac{\Delta c_p(T_g)}{k_{\rm B}}\frac{T_g}{T}\ln\frac{T_g}{T_K}\right]\frac{k_{\rm B}T}{v_{\rm int}}\right)}. \quad \textbf{[S13]}$$

Substituting the numbers in the previous paragraph, we finally obtain Eq. **4**

$$\sigma^* = \sqrt{\frac{2Gk_B T}{\kappa V_{\mathrm{bead}}}\left(\left[3.20\frac{T_K}{T} - 1.91\right] - \frac{\Delta c_p(T_g)}{k_B}\frac{T_g}{T}\ln\frac{T_g}{T_K}\right)}. \quad \text{[S14]}$$

Experimental Data and Numerical Prediction. In Table S1 we summarize the input thermodynamic data and measured strengths as well as their sources in the literature. The bead count is obtained as described by Lubchenko and Wolynes (5) and Stevenson and Wolynes (4) using the melting entropy. All strength measurements were all made at room temperature 300 K.

We also show here in Fig. S1 the comparison of measured elastic moduli with those predicted via the relation $G_{\mathrm{cal}} = 24.9k_B T_m/V_{\mathrm{bead}}$ from thermodynamic data along with the Lindemann relation and the assignment $T_A \approx T_m$. The predictions for strength use the measured G when available but use the value from Lindemann relation and $T_A \approx T_m$.

1. Stevenson JD, Schmalian J, Wolynes PG (2006) The shapes of cooperatively rearranging regions in glass-forming liquids. *Nat Phys* 2:268–274.
2. Lubchenko V, Wolynes PG (2004) Theory of aging in structural glasses. *J Chem Phys* 121:2852–2865.
3. Leath PL (1976) Cluster size and boundary distribution near percolation threshold. *Phys Rev B* 14:5046–5055.
4. Stevenson JD, Wolynes PG (2005) Thermodynamic-kinetic correlations in supercooled liquids: A critical survey of experimental data and predictions of the random first-order transition theory of glasses. *J Phys Chem B* 109:15093–15097.
5. Lubchenko V, Wolynes PG (2003) Barrier softening near the onset of nonactivated transport in supercooled liquids: Implications for establishing detailed connection between thermodynamic and kinetic anomalies in supercooled liquids. *J Chem Phys* 119:9088–9105.

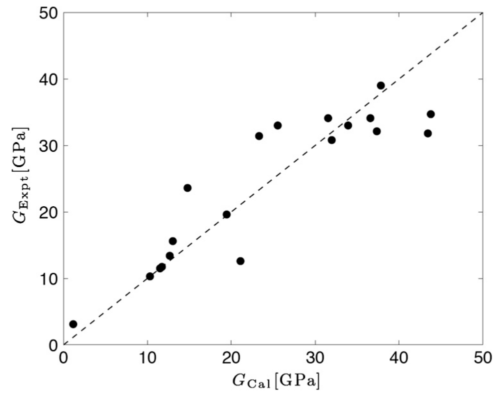

Fig. S1. Comparison between the measured elastic moduli and those calculated using the Lindemann criterion.

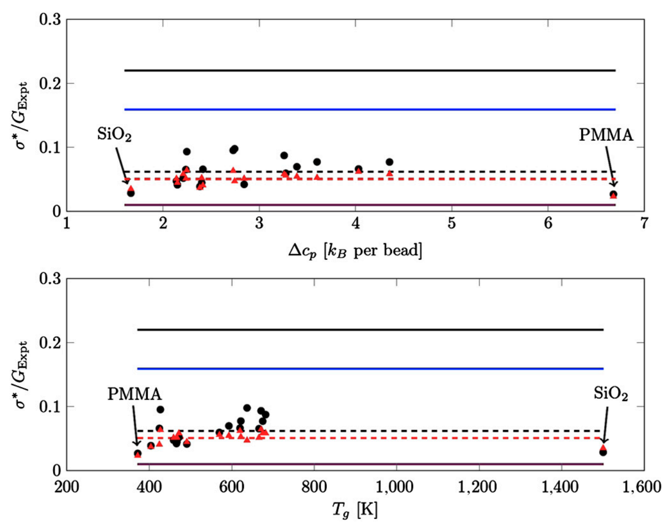

Fig. S2. The ratio between strength and shear moduli versus heat capacity change at T_g and the glass transition temperature T_g. The black circles are the RFOT theory predictions, and the red triangles are the measured values. Typical value of crystal strength (violet solid line), Frenkel strength (blue solid line), and strength in the limit $T \to 0$, $T_g \to T_K$ (black solid line) are also shown in comparison.

Table S1. Experimental data and theoretical results of 19 glasses: density $\rho(\mathrm{kg/m^3})$, latent heat of fusion ΔH_M(kJ/mol K), number of bead N_{bead}, Kauzmann temperature $T_K(K)$, glass transition temperature $T_g(K)$, melting temperature $T_M(K)$, heat capacity change at glass transition temperature Δc_p(J/mol K), experimental shear modulus G_{expt}(GPa), measured strength σ^*_{expt}(GPa), and theoretical estimated strength σ^*_{pred}(GPa)

Glasses	ρ	ΔH_M	N_{bead}	T_K	T_g	T_M	Δc_p	G_{expt}	σ^*_{expt}	σ^*_{pred}	Refs.
PMMA	1188	4.64	0.84	337	372	397	6.68	3.10	0.07	0.08	(1–7)
SiO_2	2648	9.6	0.78	876	1500	1995	1.67	31.40	1.1	0.90	(8–12)
$Mg_{65}Cu_{25}Y_{10}$	3978	8.65	0.66	325	424	771	2.41	19.60	0.8	1.29	(13–20)
$Mg_{65}Cu_{20}Zn_5Y_{10}$	3284	7.77	0.79	325	404	702	2.38	23.60	0.88	0.92	(15, 21)
$Mg_{80}Cu_{10}Y_{10}$	—	7.21	0.69	—	427	746	2.73	—	0.8	0.96	(15, 22, 23)
$La_{55}Al_{25}Ni_{20}$	6140	7.48	0.75	337	491	712	2.15	13.40	0.6	0.52	(15, 18, 19, 24, 25)
$La_{55}Al_{25}Cu_5Ni_{15}$	6050	7.51	0.82	328	472	660	2.21	—	0.6	0.47	(15, 18, 24)
$La_{55}Al_{25}Cu_{10}Ni_{10}$	5930	6.84	0.74	332	467	662	2.40	—	0.6	0.48	(15, 18, 24)
$La_{55}Al_{25}Cu_{15}Ni_5$	6370	7.21	0.78	320	459	663	2.14	—	0.6	0.52	(15, 18, 24)
$La_{55}Al_{25}Co_5Cu_{10}Ni_5$	6000	6.09	0.66	363	466	661	2.84	15.60	0.8	0.67	(15, 18, 24, 26)
$Pd_{40}Ni_{40}P_{20}$	8951	7.39	0.60	487	570	884	3.28	39	2.19	2.33	(13, 15, 18, 19, 27, 28)
$P_{40}Cu_{30}Ni_{10}P_{20}$	9300	6.84	0.61	497	593	798	3.39	33.00	1.8	2.30	(13, 15, 18, 19, 26, 29)
$Pd_{77}Cu_6Si_{17}$	10400	8.55	0.58	553	637	1058	2.74	31.80	1.5	3.11	(16, 30–32)
$Zr_{11}Cu_{27}Ni_8Ti_{34}$	6850	11.3	0.72	537	671	1128	2.25	—	2.2	3.20	(13, 18, 32–34)
$Zr_{41.2}Ti_{13.8}Ni_{10}Cu_{12.5}Be_{22.5}$	6125	8.2	0.63	553	620	937	4.03	34.10	2.12	2.26	(13, 15, 18, 2635–37)
$Zr_{46.25}Ti_{8.25}Ni_{10}Cu_{7.5}Be_{27.5}$	6014	9.4	0.57	550	622	1185	3.60	34.70	1.83	2.68	(13, 14, 16, 31, 32, 36, 38, 39)
$Zr_{52.5}Cu_{17.9}Ni_{14.6}Al_{10}Ti_5$	6730	8.2	0.55	633	675	1072	4.35	32.12	1.88	2.48	(15, 16, 18, 34, 37, 40)
$Zr_{57}Cu_{15.4}Ni_{12.6}Al_{10}Nb_5$	6690	9.4	0.62	656	682	1091	3.26	30.80	1.8	2.69	(15, 16, 18, 34, 40)
$Zr_{65}Al_{7.5}Cu_{27.5}$	6744	12.8	0.8	517	666	1150	2.24	33.00	1.7	2.16	(15, 18, 25)

1 Ute K, Miyatake N, Hatada K (1995) Glass transition temperature and melting temperature of uniform isotactic and syndiotactic poly (methyl methacrylate) s from 13mer to 50mer. *Polymer* 36:1415–1419.
2 Fernandez-Martin F, Fernandez-Pierola I, Horta A (1981) Glass transition temperature and heat capacity of heterotacticlike pmma. *J Polymer Sci Polymer Phys Ed* 19:1353–1363.
3 Prevosto D, Lucchesi M, Capaccioli S, Casalini R, Rolla P (2003) Correlation between configurational entropy and structural relaxation time in glass-forming liquids. *Phys Rev B* 67:174202.
4 Liberman S, Gomes A, Macchi E (1984) Compatibility in poly (ethylene oxide)–poly (methyl methacrylate) blends. *J Polymer Sci Polymer Phys Ed* 22:2809–2815.
5 Lee H, Paeng K, Swallen S, Ediger M (2009) Direct measurement of molecular mobility in actively deformed polymer glasses. *Science* 323:231–234.
6 Jang J, Han S (1999) Mechanical properties of glass-fibre mat/PMMA functionally gradient composite. *Compos Appl Sci Manuf* 30:1045–1053.
7 Guo Y, et al. (2012) Ultrastable nanostructured polymer glasses. *Nat Mater* 11:337–343.
8 Richet P (1984) Viscosity and configurational entropy of silicate melts. *Geochim Cosmochim Acta* 48:471–483.
9 Rabochiy P, Lubchenko V (2012) Liquid state elasticity and the onset of activated transport in glass formers. *J Phys Chem B* 116:5729–5737.
10 Bridge B, Patel ND, Waters DN (1983) On the elastic constants and structure of the pure inorganic oxide glasses. *Phys Status Solidi* 77:655–668.
11 Northolt M (1981) Compressive strength and glass transition temperature. *J Mater Sci* 16:2025–2028.
12 Bacon CR (1977) High temperature heat content and heat capacity of silicate glasses;experimental determination and a model for calculation. *Am J Sci* 277:109–135.
13 Battezzati L, Castellero A, Rizzi P (2007) On the glass transition in metallic melts. *J Non-Crystalline Solids* 353:3318–3326.
14 Busch R, Liu W, Johnson WL (1998) Thermodynamics and kinetics of the $Mg_{65}Cu_{25}Y_{10}$ bulk metallic glass forming liquid. *J Appl Phys* 83:4134–4141.
15 Cai A, Chen H, An W, Tan J, Zhou Y (2007) Relationship between melting enthalpy ΔH_m and critical cooling rate R_c for bulk metallic glasses. *Mater Sci Eng A* 457:6–12.
16 Wang WH (2012) The elastic properties, elastic models and elastic perspectives of metallic glasses. *Prog Mater Sci* 57:487–656.
17 Sheng W (2005) Evaluation on the reliability of criterions for glass-forming ability of bulk metallic glasses. *J Mater Sci* 40:5061–5066.
18 Cai A, et al. (2008) Estimation of kauzmann temperature and isenthalpic temperature of metallic glasses. *Eur Phys J B Condens Matter Complex Syst* 64:147–151.
19 Yang B, et al. (2006) Localized heating and fracture criterion for bulk metallic glasses. *J Mater Res* 21:915–922.
20 Jiang M, Dai L (2007) Intrinsic correlation between fragility and bulk modulus in metallic glasses. *Phys Rev B* 76:054204.
21 Hui X, et al. (2006) In-situ $Mg_{77}Cu_{12}Zn_5Y_6$ bulk metallic glass matrix composite with extraordinary plasticity. *Chin Sci Bull* 51:229–234.
22 Murty B, Hono K (2000) Formation of nanocrystalline particles in glassy matrix in melt-spun mg-cu-y based alloys. *Mater Trans JIM (Japan)* 41:1538–1544.
23 Inoue A, Zhang W, Zhang T, Kurosaka K (2001) High-strength cu-based bulk glassy alloys in Cu–Zr–Ti and Cu–Hf–Ti ternary systems. *Acta Mater* 49:2645–2652.
24 Lu Z, Li Y, Liu C (2003) Glass-forming tendency of bulk La–Al–Ni–Cu–(Co) metallic glass-forming liquids. *J Appl Phys* 93:286–290.
25 Perera D (1999) Compilation of the fragility parameters for several glass-forming metallic alloys. *J Phys Condens Matter* 11:3807–3812.
26 Johnson WL, Samwer K (2005) A universal criterion for plastic yielding of metallic glasses with a $(T/T_g)^{2/3}$ temperature dependence. *Phys Rev Lett* 95:195501.
27 Hu X, Tan T, Li Y, Wilde G, Perepezko J (1999) The glass transition of $Pd_{40}Ni_{10}Cu_{30}P_{20}$ studied by temperature-modulated calorimetry. *J Non-crystalline Solids* 260:228–234.
28 Yu H, Wang W, Bai H (2010) An electronic structure perspective on glass-forming ability in metallic glasses. *Appl Phys Lett* 96:081902.
29 Lu Z, Tan H, Li Y, Ng S (2000) The correlation between reduced glass transition temperature and glass forming ability of bulk metallic glasses. *Scripta Mater* 42:667–674.
30 Komatsu T (1995) Application of fragility concept to metallic glass formers. *J Non-crystalline Solids* 185:199–202.
31 Cai A, Sun G, Pan Y (2006) Evaluation of the parameters related to glass-forming ability of bulk metallic glasses. *Mater Des* 27:479–488.
32 Lu ZP, Liu CT (2002) A new glass-forming ability criterion for bulk metallic glasses. *Acta Mater* 50:3501–3512.
33 Bossuyt S (2001) Microstructure and crystallization behavior in bulk glass forming alloys. Ph.D. thesis (California Institute of Technology, Pasadena, CA).
34 Glade SC, et al. (2000) Thermodynamics of $Cu_{47}Ti_{34}Zr_{11}Ni_8$, $Zr_{52.5}Cu_{17.9}Ni_{14.6}Al_{10}Ti_5$ and $Zr_{57}Cu_{15.4}Ni_{12.6}Al_{10}Nb_5$ bulk metallic glass forming alloys. *J Appl Phys* 87:7242–7248.
35 Busch R, Kim YJ, Johnson WL (1995) Thermodynamics and kinetics of the undercooled liquid and the glass transition of the $Zr_{41.2}Ti_{13.8}Cu_{12.5}Ni_{10}Be_{22.5}$ alloy. *J Appl Phys* 77:4039–4043.
36 Wang W, Dong C, Shek C (2004) Bulk metallic glasses. *Mater Sci Eng R Rep* 44:45–89.
37 Wang J, Choi B, Nieh T, Liu C (2000) Crystallization and nanoindentation behavior of a bulk Zr–Al–Ti–Cu–Ni amorphous alloy. *J Mater Res* 15:798–807.
38 Demetriou M, Johnson W, Samwer K (2009) Rheology and ultrasonic properties of metallic glass-forming liquids. *J Alloy Comp* 483:650–654.
39 Wiest A (2010) Thermoplastic forming and related studies of the supercooled liquid region of metallic glasses. Ph.D. thesis (California Institute of Technology, Pasadena, CA).
40 Pang J, Tan M, Liew K (2012) On valence electron density, energy dissipation and plasticity of bulk metallic glasses. *J Alloy Comp*, 10.1016/j.jallcom.2012.03.036.